



Sealed-off helium-filled proportional counter for the conversion electron Mössbauer spectroscopy

Taizo Kawauchi¹ · Kanta Asakawa¹ ·
Katsuyuki Fukutani¹

© Springer International Publishing AG 2017

Abstract Conversion electron Mössbauer spectroscopy (CEMS) is a surface-sensitive technique because of the shallowness of the escape depth of conversion electrons. The proportional counter with the sample built-in is usually used for CEMS with a flow of He mixed with a quenching gas. This flow-type proportional counter with a mixed gas, however, is not suited to high-temperature measurements. For high-temperature operation, we fabricated a sealed-off proportional counter operated above 850 K for CEMS, which is filled with pure He at a pressure of $1\text{--}8 \times 10^4$ Pa. The distribution of the output pulse voltage revealed an inflection point suggesting that two multiplication mechanisms are operative. The multiplication factor of the proportional counter was estimated to be about $10^4\text{--}10^5$. By means of the fabricated proportional counter, we investigated the magnetic phase transition of Fe_3O_4 , whose Curie temperature is 858 K. We successfully observed the ferromagnetic-paramagnetic phase transition without the reduction of the sample.

Keywords Sealed-off proportional counter · Conversion electron Mössbauer spectroscopy · High-temperature operation

This article is part of the Topical Collection on *Proceedings of the International Conference on the Applications of the Mössbauer Effect (ICAME 2017), Saint-Petersburg, Russia, 3–8 September 2017*
Edited by Valentin Semenov

✉ Taizo Kawauchi
kawauchi@iis.u-tokyo.ac.jp

Kanta Asakawa
asakawa@issp.u-tokyo.ac.jp

Katsuyuki Fukutani
fukutani@iis.u-tokyo.ac.jp

¹ Institute of Industrial Science, The University of Tokyo, 4-6-1, Komaba, Meguro-ku, Tokyo 153-8505, Japan

1 Introduction

Conversion electron Mössbauer spectroscopy (CEMS) is a surface-sensitive technique for investigation of the magnetic properties and chemical states of materials, because the probing depth of conversion electrons is less than 100 nm [1]. For the detailed analysis of the sample, e.g. the critical phenomena of the sample surfaces, it is often required to measure the temperature dependence of CEMS. For a wide-range-temperature operation, in-situ depth selective CEMS (DCEMS) in ultra-high vacuum was developed [2, 3]. However, because this method uses an electron energy analyzer with an acceptance angle of $\sim 0.2\pi$ and an electron detector with a detection efficiency of $\sim 10\%$ with respect to the FeK-shell conversion electron of 7.3 keV, the detection efficiency of this method is a few percent of that of the conventional CEMS by using the proportional counter with the sample built-in [4]. Moreover, the conventional CEMS by means of the proportional counter using mixture of inert gas and hydrocarbon gas is not appropriate to apply to the system that suffers from the reaction of the sample with hydrocarbon at high temperature [5]. A proportional counter available to such reactive systems remains to be developed. For high-temperature operation, the proportional counter needs to be sealed off at a reduced pressure for the stability of the sample temperature and to be filled with pure inert gas without quench gas because the amount of the quench gas is gradually reduced due to dissociation

The characteristics of the proportional counter as a detector for photons and charged particles has been investigated in detail [6, 7]. The signal pulse is obtained by the multiplication effect of the gas ionization, which is caused by the electric potential gradient in the detector. The proportional counter often uses mixture of host gas for ionization and a polyatomic molecule gas for quenching metastable He atoms to avoid the discharge [8–12]. When He is mixed with a polyatomic molecule gas such as CH₄, the metastable He atom is quenched by collision with CH₄ without additional secondary-electron emission, because the dissociation energy of 4.5 eV for CH₄ is lower than the energy between the metastable and ground states of He [13, 14]. At low temperature, however, the proportional counter can be operative with pure He without the quenching gas [15, 16]. Below 20 K, He_n⁺ ($n=3-30$) clusters are formed, which dissociate by receiving an energy from the metastable He quenching it to the ground state [17].

On the other hand, if the collector anode potential is kept sufficiently low to suppress the generation of metastable He atoms, the pure-He proportional counter might be operative [18, 19]. In exchange for suppression of the discharge, the gas-multiplication coefficient is decreased because of the low electric field. The turning point whether the counter works as a detector or not is that the required voltage applied to the collector electrode to obtain the signal pulse electron is lower than the discharge voltage or not [15, 20]. In our previous work, we confirmed that the CEMS spectrum can be measured with pure He at room temperature preventing discharge [21]. Although the discharge voltage certainly decreased due to the disappearance of the effect of the cluster, there is the region where the applied electric field to obtain amplification is lower than the discharge voltage.

In this work, a sealed-off proportional counter with pure He at a reduced pressure is designed in consideration of the threshold of the electric field near the collector electrode for electron-avalanche multiplication and discharge electric field. The achieved multiplication factor of the home-made proportional counter was estimated at $2-6 \times 10^4$. The output pulse-height-distribution as a function of the voltage reveals an inflection, which suggests that there are two multiplication processes. By means of the fabricated proportional counter, we measured the temperature dependence of CEMS for Fe₃O₄. As a result, we successfully

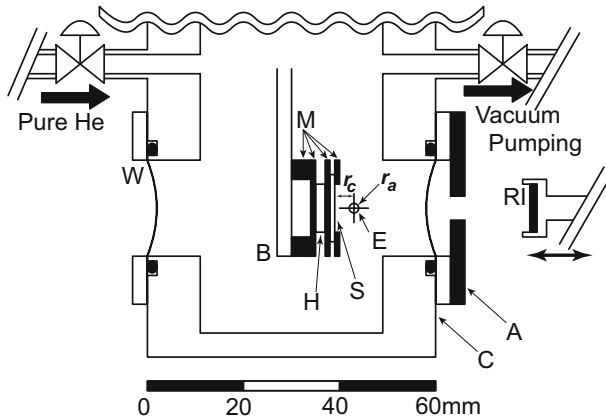


Fig. 1 Configuration of the fabricated sealed-off proportional counter. A: 3mm-thick lead aperture with a diameter of $\phi 5$ mm, B: copper base plate of the sample holder, C: main chamber of the proportional counter, E: collector electrode of a gold wire with a diameter of $\phi 100 \mu\text{m}$, H: a ceramic heater, M: molybdenum sample holder assembly, RI: ^{57}Co radioisotope, r_a : radius of collector, r_c : distance between the collector and the sample, S: sample, W: $125 \mu\text{m}$ -thick polyimide window

measured the CEMS spectrum up to 871 K and observed the magnetic phase transition at the Curie temperature [22] without the reduction of the sample.

2 Apparatus

Two key points for designing the pure-He proportional counter are the sufficient multiplication and suppression of discharge. Whereas the threshold of the electric field in the vicinity of the collector electrode for electron-avalanche multiplication E_A is $\sim 10^4 \text{ V/cm}$ [23], the discharge electric-field in He E_D is lower than $\sim 8 \times 10^3 \text{ V/cm}$ [24]. The electric field $E(r)$ at a distance r from the center of the collector electrode is described as

$$E(r) = V / (r \ln(r_c / r_a)), \tag{1}$$

where V , r_c and r_a are the voltage applied to the collector, the distance between the sample and the center of the collector and the radius of the collector, respectively [23].

To avoid the discharge, the electric field V/r_c should be smaller than E_D . As a result, r_c and r_a were set 3 mm and 0.05 mm, respectively, and the applied voltage was set in the range from 240 to 680 V. The electric field is estimated in the range from 6×10^2 to $2 \times 10^3 \text{ V/cm}$. The electric field near the collector electrode is, on the other hand, as large as E_A , which potentially allows for sufficient multiplication.

The configuration of the fabricated proportional counter is shown in Fig. 1. The detector chamber is made of stainless steel whose size is $5 \times 6 \times 7 \text{ cm}^3$ and the volume of the internal space is 120 cm^3 . The window material to introduce the γ -ray from the ^{57}Co source is polyimide, which is stable up to 600 K and has the permeability for nitrogen and oxygen of 1.3×10^{-15} and $5.4 \times 10^{-15} \text{ mol} \cdot \text{m}^{-2} \cdot \text{s}^{-1} \cdot \text{Pa}^{-1}$, respectively (http://www.td-net.co.jp/kapton/sort/hv_type/chemical.html). Previous reports also used an insulator for the window to measure CEMS although the reason is not specified [16, 25]. Since a slight increase in the gaseous impurity of 0.1 at% in a proportional counter significantly decreases the gain of

the output pulse [26], the polyimide films were carefully fixed with o-rings, where the leak and outgas rate was estimated to be less than $10^{-10}\text{Pam}^3\text{s}^{-1}$. A lead aperture was placed as shown in Fig. 1 to avoid the paramagnetic signal from the stainless steel.

After pumping with a turbo molecular pump, the chamber was filled with 99.995% pure He at several pressures higher than 10^4 Pa. A ceramic heater set at the back side of the sample was used for sample heating, and the sample temperature was monitored by a thermocouple. The signal from the collector electrode was amplified by a charge-sensitive amplifier whose sensitivity was -290 mV/pC and an amplifier whose gain was 200. To pick up the signal, we reduced the noise level of the output from the preamplifier down to 1 mV.

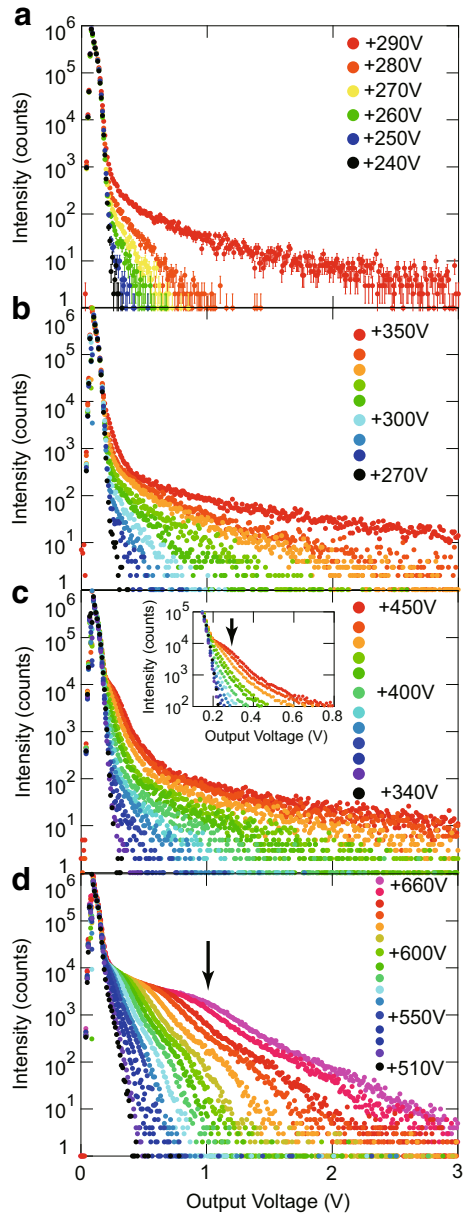
3 Results

3.1 Output characteristics

The output characteristics of the proportional counter measured for an α -Fe foil at room temperature with an acquisition time of 150 s are shown in Figs. 2 and 3. Figure 2a–d shows the distributions of the output pulse voltage after amplification at several collector-bias voltages and He pressures of $1\text{--}8 \times 10^4$ Pa. The signal below 0.2 eV in Fig. 2 is the background. The output voltage increases with the elevation of the bias voltage applied to the collector electrode. In Fig. 2a–c, there is an inflection point where the slope largely changes, e.g. at 0.4 V for +350 V in Fig. 2b and at 0.7 V for 450 V in Fig. 2c. This suggests that the charge multiplication mechanism changes at this inflection point. The charge multiplication is caused by either the Taunsent ionization or He ionization by collision between metastable He atoms, and the multiplication factor due to the latter is expected to be larger than the former [18, 27, 28]. Therefore, it is considered that the component below the inflection point is caused by Taunsent ionization, which is direct ionization of He by the impact of electrons and contributes to the amplification factor from 10^4 to 10^5 . On the other hand, it is considered that the other component above the inflection point is caused by ionization due to collision between the metastable He atoms, which contributes to the amplification factor of the order of 10^5 . A previous study with a proportional counter using pure He at low temperature observed the energy spectrum corresponding to the K conversion electrons and Auger electrons. It is noted that there is a hump below the inflection point as indicated by arrows in Fig. 2. Since the present detector is not designed for energy-resolved detection, the K-conversion electron is not resolved from Auger electrons and might be observed as a hump in the spectrum [29].

The multiplication factor is estimated by the mean value of these output-pulse-height distributions in consideration of the gain of the amplifier and the charge-sensitivity of the preamplifier as shown in Fig. 3. In Fig. 3, at each pressure of He, the amplification factor is increased with increasing potential applied to the collector electrode. At all He pressures, the amplification factor is estimated to be $2 - 6 \times 10^4$. The operation voltage becomes high when the He pressure increases. In previous work, it is investigated that the customary region of the proportional counter is $E/p \lesssim 1$ V/cm·Pa, where E and p are the electric field and the gas pressure, and that the gas-amplification factor is in the range from 10^4 to 10^5 [30]. In the present work, E/p is in the range from 10^{-2} to 10^{-1} V/cm·Pa, which is smaller than the customary region of the proportional counter. On the other hand, the amplification factor in Fig. 3 compares favourably with the customary proportional counter. At this stage, the reason is not clear why the amplification factor is sufficiently large to detect the signal in spite of small E/p . As a possible reason, it is considered that the ionization caused by the

Fig. 2 Pulse height distributions of the output pulse at He pressures of **a** 1×10^4 , **b** 2×10^4 , **c** 4×10^4 and **d** 8×10^4 Pa. The bias voltages applied to the collector electrode are indicated in each graph. The inset in **c** is the close-up in the range of output voltage from 0.1 to 0.8 V. The accumulating time of each data was 150 sec. The humps in the spectra of **c** and **d** are indicated by arrows



metastable He atom contributes to the amplification under the condition that the discharge is suppressed.

3.2 Measurement of CEMS

Figure 4 shows the CEMS spectrum of an α -Fe foil by means of the fabricated proportional counter at a He pressure of 4×10^4 Pa. The internal magnetic field, the isomer shift and

Fig. 3 Bias dependence of the gas-multiplication factor at pressures of 5×10^3 (\blacktriangle), 1×10^4 (\square), 2×10^4 (\blacksquare), 4×10^4 (\circ) and 8×10^4 Pa (\bullet)

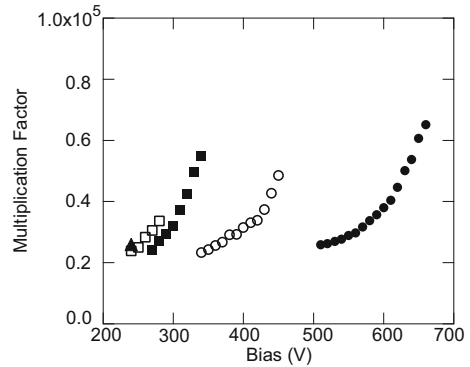
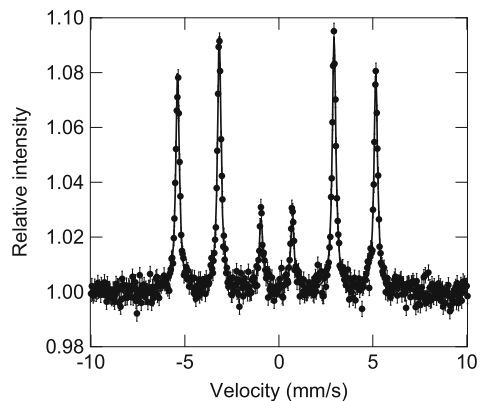


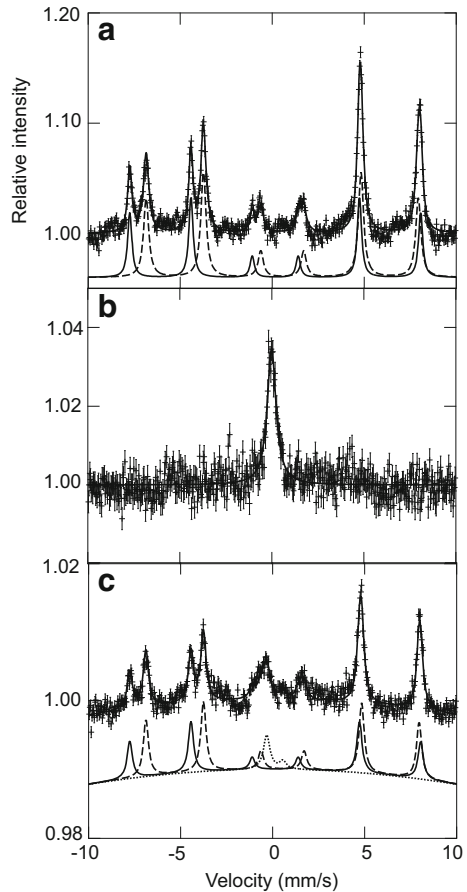
Fig. 4 CEMS spectrum of an α -Fe foil at a He pressure of 4×10^4 Pa and at room temperature. The voltage applied to the collector is 680 V, and the accumulation time is 4 days



the line width are estimated at 32.69 ± 0.01 T, -0.001 ± 0.001 mm/s and 0.232 ± 0.004 mm/s, respectively. The velocity zero is defined as the center of the α -iron spectrum. The isomer shift and the line width of ^{57}Co in a Rh matrix are -0.11 and 0.234 mm/s, respectively. Therefore, it is confirmed that the CEMS spectrum of α -Fe is successfully measured. The relative intensity of α -Fe in Fig. 4 is comparable to that measured with a conventional He+CH₄ gas-flow proportional counter.

The CEMS spectra of Fe₃O₄(100) are shown in Fig. 5a–c. The surface of the Fe₃O₄(100) sample used in the present study is ^{57}Fe -enriched with a thickness of 20 nm by homoepitaxial growth on the Fe₃O₄(100) single-crystal surface. The procedure of the sample preparation is described in our previous study [31]. In Fig. 5a, the spectrum at room temperature clearly reveals the two sites of Fe₃O₄, whose hyperfine magnetic fields B_{hf} and isomer shifts δ_{IS} are ($B_{hf1}=49.03 \pm 0.02$ T, $\delta_{IS1}=0.277 \pm 0.003$ mm/s) and ($B_{hf2}=45.87 \pm 0.02$ T, $\delta_{IS2}=0.659 \pm 0.003$ mm/s). These values are in good agreement with previous data [32]. At 871 K, which is above the Curie temperature of Fe₃O₄ [22], a paramagnetic phase is observed as shown in Fig. 5b. When the sample is cooled from 871 K to room temperature, the magnetic phase is restored and an additional paramagnetic component appears as seen in Fig. 5c. The isomer shift of -0.209 ± 0.059 mm/s of the paramagnetic component in Fig. 5c is different from that of $+0.10 \pm 0.01$ mm/s in Fig. 5b. It is considered that the additional component is different from FeO and might be attributed to the iron trapped at the interstitial site in Fe₃O₄ [33–35]. It is worth pointing out that the reduction of the surface is

Fig. 5 CEMS spectra of $^{57}\text{Fe}_3\text{O}_4(20\text{nm})/\text{Fe}_3\text{O}_4$ as-deposited at **a** 293 K, **b** at 871 K and **c** at 294 K cooled from 871 K at a He pressure of 5.5×10^4 Pa. The voltage applied to the collector is 460 V. The accumulation times are **a** 5 days, **b** 17 hours and **c** 5 days. Solid and broken curves in **a** and **b** are the fits for the tetrahedral and octahedral sites of Fe, respectively



not caused by heating at 871 K. The relative intensity of Fe_3O_4 in Fig. 5c is decreased compared to that in Fig. 5a. This is probably because ^{57}Fe in the $^{57}\text{Fe}_3\text{O}_4$ layer diffused into Fe_3O_4 bulk [36]. Note that the background seems to be enhanced around 0 mm/s in Fig. 5c. This is probably because the vertical scale is expanded compared to that of Fig. 5a and the RI position is closest to the sample at 0 mm/s for the velocity modulation.

4 Conclusion

A sealed-off He-filled proportional counter is fabricated for CEMS with the sample built-in by taking into consideration the threshold electric field for electron multiplication and discharge. The proportional counter is found to be operative at a He pressure of $1\text{--}8 \times 10^4$ Pa without a quench gas, and the multiplication factor is estimated to be $2\text{--}6 \times 10^4$. With this proportional counter, the CEMS is successfully measured for Fe_3O_4 at a high temperature, which reveals a paramagnetic phase above the Curie temperature of 858 K. It is also confirmed that the reduction of the surface did not occur upon high-temperature measurement in the range of the probing depth of 100 nm.

References

1. Thomas, J., Tricker, M., Winterbottom, A.: Conversion electron Mössbauer spectroscopic study of iron containing surfaces. *J. Chem. Soc. Faraday Trans. II*(71), 1708 (1975)
2. Shigematsu, T., Pfannes, H., Keune, W.: Depth-selective conversion electron Mössbauer spectroscopy. *Phys. Rev. Lett.* **45**, 1206 (1980)
3. Korecki, J., Gradmann, U.: In situ Mössbauer analysis of hyperfine interactions near Fe(110) surfaces and interfaces. *Phys. Rev. Lett.* **55**, 2491 (1985)
4. Kruijer, S., Nikolov, O., Keune, W., Reuther, H., Weber, S., Scherrer, S.: Depth analysis of phase formation in α -Fe after high dose Al ion implantation. *J. Appl. Phys.* **84**, 6570 (1998)
5. Sharma, S., Nomura, K., Ujimura, Y.: Mössbauer studies on tin-bismuth oxide CO selective gas sensor. *J. Appl. Phys.* **71**, 2000 (1992)
6. Rose, M., Korff, S.: An investigation of the properties of proportional counters. I. *Phys. Rev.* **59**, 850 (1941)
7. Korff, S.: The operation of proportional counters. *Rev. Mod. Phys.* **14**, 1 (1942)
8. Ramsey, B., Agrawal, P.: Quench gases for Xenon- (and Krypton-) filled proportional counters. *Nucl. Instrum. Meth. Phys. Res. A* **273**, 326 (1988)
9. Agrawal, P., Ramsey, B.: Use of propane as a quench gas in argon-filled proportional counters and comparison with other quench gases. *Nucl. Instrum. Meth. Phys. Res. A* **273**, 331 (1988)
10. Petkau, K., Hammer, J., Herre, G., Mantel, M., Langhoff, H.: Vacuum ultraviolet emission spectra of the helium and neon alkali ions in the range between 60–80 nm. *J. Chem. Phys.* **94**, 7769 (1991)
11. Found, C.: Ionization potentials of argon, nitrogen, carbon monoxide, helium, hydrogen and mercury and iodine vapors. *Phys. Rev.* **16**, 41 (1920)
12. Lowry, J., Tombouliau, D., Ederer, D.: Photoionization cross section of helium in the 100- to 250-Å Region. *Phys. Rev.* **137**, A1054 (1965)
13. Isozumi, Y., Kurakado, M., Katano, R.: A proportional counter for resonance conversion-electron Mössbauer spectroscopy at low temperatures down to 77.3 K. *Nucl. Instrum. Meth.* **204**, 571 (1983)
14. Schmeltekopf, A., Fehsenfeld, F.: De-excitation rate constants for Helium metastable atoms with several atoms and molecules. *J. Chem. Phys.* **53**, 3173 (1970)
15. Isozumi, Y., Ito, S., Fujii, T., Katano, R.: Helium-filled proportional counter for low-temperature operation(1.75–4.2K) and application to cryogenic resonance-electron Mössbauer spectroscopy II. *Rev. Sci. Instrum.* **60**, 3262 (1989)
16. Cook, D., Agyekum, E.: Gas flow proportional counter for low temperature conversion electron Mössbauer spectroscopy. *Nucl. Instrum. Meth. Phys. Res. B* **12**, 515 (1985)
17. Haberland, H., Issenforff, B., Fröchtenicht, R., Toennis, J.: Absorption spectroscopy and photodissociation dynamics of small helium cluster ions. *J. Chem. Phys.* **102**, 8773 (1995)
18. Deloche, R., Monchicourt, P., Cheret, M., Lambert, F.: High-pressure helium afterglow at room temperature. *Phys. Rev. A* **13**, 1140 (1976)
19. Dugan, J., Richards, H., Muschlitz, E. Jr.: Excitation of the metastable states of helium by electron impact. *J. Chem. Phys.* **46**, 346 (1967)
20. Kishimoto, S., Isozumi, Y., Katano, R., Takekoshi, H.: Operation of Helium-filled proportional counter at low temperatures (4.2–295K). *Nucl. Instrum. Meth. Phys. Res. A* **262**, 413 (1987)
21. Kawachi, T., Nagatsuka, N., Fukutani, K.: Observation of photoexcitation of Fe-oxide grown on TiO₂(100) by visible light irradiation. *Hyp. Int.* **237**, 73 (2016)
22. Levy, D., Guistetto, R., Hoser, A.: Structure of magnetite (Fe₃O₄) above the Curie temperature: a cation ordering study. *Phys. Chem. Miner.* **39**, 169 (2012)
23. Matoba, M., Hirose, T., Sakae, T., Kametani, H., Ijiri, H., Shintake, T.: Three dimensional Monte Carlo simulation of the electron avalanche around an anode wire of a proportional counter. *IEEE Trans. Nucl. Sci.* **NS-32**, 541 (1985)
24. Ivković, S., Obradović, B., Cvetanović, N., Kuracia, M., Purić: Measurement of electric field development in dielectric barrier discharge in helium. *J. Phys. D* **42**, 225206 (2009)
25. Mantvan, R., Faucilli, M.: Development of a parallel-plate avalanche counter to perform conversion electron Mössbauer spectroscopy at low temperatures. *Rev. Sci. Instrum.* **78**, 063902 (2007)
26. Aponte, J., Korff, S.: Effect of gaseous impurities on BF₃ proportional counters. *Rev. Sci. Instrum.* **31**, 532 (1960)
27. Wetzel, W.: The quantum mechanical cross section for ionization of helium by electron impact. *Phys. Rev.* **44**, 25 (1933)
28. Kruithof, A., Penning, F.: Determination of the Townsend ionization coefficient α for pure Argon. *Physica* **3**, 515 (1936)

29. Fukumura, K., Katano, R., Kobayashi, T., Nakanishi, A., Isozumi, Y.: Helium-filled proportional counter operated at low temperatures higher than 13 K. *Nucl. Instrum. Meth. Phys. Res. A* **301**, 482 (1991)
30. Gold, R., Bennet, E.: Electron multiplication process in proportional counters. *Phys. Rev.* **147**, 201 (1966)
31. Asakawa, K., Kawauchi, T., Zhang, X., Fukutani, K.: Non-collinear magnetic structure on the $\text{Fe}_3\text{O}_4(111)$ surface. *J. Phys. Soc. Jpn.* **86**, 074601 (2017)
32. Murad, E., Johnson, J.: Mössbauer spectroscopy applied to inorganic chemistry. In: Long, G. (ed.), vol. 2, p. 507. Plenum Press, New York (1984)
33. Gohy, C., Gérard, A., Grandjean, F.: Mössbauer study of Wustite and Mangano-Wustite. *Phys. Stat. Sol. A* **74**, 583 (1982)
34. Becker, K., Wurmb, V.: Mössbauer study of high-temperature diffusion in magnetite. *Hyp. Int.* **56**, 1431 (1990)
35. Wißmann, S., Wurmb, V., Litterst, F., Dieckmann, R., Becker, K.: The temperature-dependent cation distribution in magnetite. *J. Phys. Chem. Sol.* **59**, 321 (1998)
36. Atkinson, A., O'Dwyer, M., Taylor, R.: ^{55}Fe diffusion in magnetite crystals at 500 °C and its relevance to oxidation of iron. *J. Mat. Sci.* **18**, 2371 (1983)